JOURNAL OF AIRCRAFT
Vol. 33, No. 1, January–February 1996

Integrated Determination of Sensitivity Derivatives for an Aeroelastic Transonic Wing

Alan E. Arslan* and Leland A. Carlson†
Texas A&M University, College Station, Texas 77843-3141

The incremental iterative technique is used to effectively couple for three-dimensional transonic flow about a twisted unswept rectangular wing, an aerodynamic solution for the pressure distribution with a structural solution for the corresponding deflections and, using the quasianalytical approach, simultaneously obtain the aerodynamic, structural, and coupling sensitivity derivatives for the fully coupled system. The solution includes aerodynamic sensitivities for nine design variables at all flowfield points, structural sensitivities for four design variables at 490 points on the wing, and 450 coupling sensitivities. Subsequently, fully coupled system sensitivity derivatives are obtained. The results often show significant differences between the discipline and system sensitivity derivatives and that the system derivatives are sensitive to the location and number of coupling derivatives.

Nomenclature

C = maximum camber
C_l = section lift coefficient
C_p = pressure coefficient
d( )/d( ) = system sensitivity derivative
E = Young's modulus of elasticity
LC = location of maximum camber
M_∞ = freestream Mach number
R = residual of the aerodynamic equation
T = residual of the structural equation
TH = maximum thickness
T_{tip} = twist angle at the tip
t = thickness of the plate
U_∞ = freestream velocity, also U_{inf}
XD = vector of design variables
x, y, z = Cartesian coordinate directions
α = angle of attack
γ = ratio of specific heats
ΔC_p = $C_{pl} - C_{pu}$
δ = structural deflections
ν = Poisson's ratio
ρ_∞ = freestream density
ϕ = small perturbation velocity potential function
$\partial( )/\partial( )$ = discipline sensitivity derivative

Subscripts

A = obtained from aerodynamic variables alone
i, j, k = grid point
l = lower side of the wing
l, m, n = grid point
root = at the wing root
S = obtained from the structural variables alone
tip = at the wingtip
u = upper side of the wing

Presented as Paper 94-4400 at the AIAA/USAF/NASA/ISSMO 5th Symposium on Multidisciplinary Analysis and Optimization, Panama City Beach, FL, Sept. 7–9, 1994; received Oct. 11, 1994; revision received July 26, 1995; accepted for publication Aug. 11, 1995.

*Graduate Research Assistant, Department of Aerospace Engineering. Student Member AIAA.
†Professor, Department of Aerospace Engineering. Associate Fellow AIAA.

Introduction

IN the nonlinear transonic regime, the determination of optimum aerodynamic loads is one of the main difficulties facing the aircraft designer, and today computational methods that use optimization techniques are being developed to improve current designs. However, for such advanced approaches to become more useful as design tools, it is necessary to develop methods for the computation of the sensitivity of the different parameters, such as aerodynamic forces or structural deflections, to the different design variables.

In the past, sensitivity methodology has been used in structural design[1] and optimization programs[2] and in some aerodynamic studies.[3–8] However, a significant contributor to required computational resources in gradient based optimization procedures has often been the calculation of sensitivity derivatives. Hence, efficient numerical methods for computing such derivatives are needed, particularly in three dimensions where the computational resources for a single flow analysis can be extremely high. In addition, optimization, particularly aerodynamic, often requires the modification of pressures in a specific region. Thus, local sensitivity derivatives of C_p with respect to the design variables are often needed as well as global derivatives involving integrated values such as lift coefficients, etc. Again, methods for obtaining these local sensitivities are needed. Finally, for an optimization process to be accurate, it must have available system sensitivity derivatives in which the effects of each discipline on the other are considered.

Sensitivity derivatives can, in principle, be computed by direct differentiation of the governing equations. In the case where the continuous governing equations are differentiated prior to their numerical discretization, the method is known as the continuum or the analytical approach.[3] On the other hand, if the governing equations are differentiated after their discretization, the method is known as the discrete or the quasianalytical approach.

Investigations concerning the feasibility of the quasianalytical approach for the computation of the aerodynamic sensitivity derivatives have been undertaken by many researchers[3–7] and several methods have proven to be very successful. However, the differentiation of the governing discretized equations results in very large systems of algebraic linear sensitivity equations that must be solved to obtain the derivatives of interest. The application of a direct solver method to such a system requires extensive computer storage, which for practical three-dimensional problems is beyond the capacity of most machines.[5] Moreover, the sensitivity matrix, sparse in nature,

is sometimes ill conditioned (or not diagonally dominant), and the convergence by the use of standard iterative techniques is slow.[7] To avoid these problems, it is necessary to develop other iterative solution algorithms of the sensitivity equations. One possibility is the incremental iterative technique[3,7] that allows the iterative calculation of the sensitivity derivatives using algorithms similar to those applied to the flowfield.

The incremental iterative technique can be applied through a point semi-implicit algorithm to solve simultaneously for the flowfield, structural deflections, and their respective sensitivities with respect to the different design variables. However, these results are only discipline specific, and the effect of one discipline on the sensitivity derivatives of the other[8] needs to be considered. In other words, system as well as discipline derivatives need to be determined.

Consequently, the primary objective of this proof-of-concept effort is to investigate the concept that it is possible to use similar, perhaps identical, incremental iterative solution approaches to couple for three-dimensional transonic flow, an aerodynamic solution with a structural solution, and to simultaneously use the same solution algorithms to obtain the aerodynamic and structural discipline sensitivity derivatives for the fully coupled system along with the coupling derivatives necessary to determine system sensitivities. A secondary objective is to study the number and location of the coupling derivatives needed to determine system sensitivities.

Theory

Flowfield Model

The equations governing transonic flow are nonlinear and range from the Navier–Stokes equations to the small perturbation potential equation. Since this study is a proof-of-concept investigation, the flow modeling is the simplest possible, e.g., the nonconservative nonlinear transonic small perturbation equation:

$$[1 - M_\infty^2 - (\gamma + 1)M_\infty^2\phi_x]\phi_{xx} + \phi_{yy} + \phi_{zz} = 0 \qquad (1)$$

with the x axis downstream, y axis up, and the z axis in the spanwise direction, and the usual surface, wake, and far-field boundary conditions.[9,10]

The finite differencing of Eq. (1), requires the use of a residual R written in functional notation at the point i, j, k as

$$R_{i,j,k} = R_{i,j,k}(\phi_{l,m,n}, \boldsymbol{XD}) \qquad (2)$$

Since the structural deflections are included in the boundary conditions and are not treated as dependent design variables in the previous equation, Eq. (2) should be considered a discipline equation.

After taking the total differential of Eq. (2) with respect to a specific design variable $\boldsymbol{XD}$, the sensitivity equation is obtained:

$$\frac{dR_{i,j,k}}{dXD} = \left[\frac{\partial R_{i,j,k}}{\partial \phi_{l,m,n}}\right]\left\{\frac{\partial \phi_{l,m,n}}{\partial XD}\right\} + \left\{\frac{\partial R_{i,j,k}}{\partial XD}\right\} = 0 \qquad (3)$$

In this equation lies the essence of the quasianalytical formulation in which the discretized governing equations are differentiated. Here, $\phi_{l,m,n}$ is $\phi[x(l), y(m), z(n), \boldsymbol{XD}, \boldsymbol{\delta}]$; and the system matrix $\partial R/\partial\phi$ is sparse or nonzero only at certain points (mostly the ones neighboring i, j, k). In this equation, the vector of deflections $\{\boldsymbol{\delta}\}$, even though not explicitly shown, is considered to be a vector of independent variables. Near the boundaries, Eq. (3) has been reformulated to include the flowfield boundary conditions. The flowfield sensitivity derivatives $\partial\boldsymbol{\phi}/\partial\boldsymbol{XD}$ that are obtained from solving Eq. (3) can be used to calculate pressure sensitivities $\partial C_p/\partial\boldsymbol{XD}$, which in turn can be used to calculate the sensitivities of the section and wing lift to the design variables.

Structural Modeling

To keep the problem simple and to permit rapid solutions, the wing structure is modeled by an equivalent flat plate with dimensions almost coincident with those of the wing. The equation describing the plate deflections is

$$[Et^3/12(1 - \nu^2)]\nabla^4\delta - \tfrac{1}{2}\rho_\infty U_\infty^2 \Delta C_p = 0 \qquad (4)$$

which assumes a thin plate and small deflections. This model, while simple, will yield both bending and twisting effects.

The boundary conditions for Eq. (4) involve both fixed and free edges. The root is the only fixed edge and there the boundary condition is no deflection and zero spanwise slope. At the wingtip, leading-, and trailing-edges differential equation boundary conditions representing no twisting moment, no shearing force, and zero bending moment were utilized.[9,10]

The residual for Eq. (4) can be expressed as

$$T_{i,k} = T_{i,k}(\delta_{l,n}, \boldsymbol{XD}) \qquad (5)$$

Again, this equation is discipline specific since $\delta_{l,n} = \delta[x(l), z(n), \boldsymbol{\phi}_{l,n}, \boldsymbol{XD}]$; and $\boldsymbol{\phi}_{l,n}$ is the vector of potentials on the upper and lower side of the wing that are related to the calculation of loads. This vector is considered to be composed of independent variables. Unlike the flowfield case, which is three dimensional, the deflection field is a two-dimensional variable.

After taking the total derivative of Eq. (5) with respect to a specific design variable, the structural sensitivity equation is obtained:

$$\frac{dT_{i,k}}{dXD} = \left[\frac{\partial T_{i,k}}{\partial \delta_{l,n}}\right]\left(\frac{\partial \delta_{l,n}}{\partial XD}\right) + \left(\frac{\partial T_{i,k}}{\partial XD}\right) = 0 \qquad (6)$$

In this case, also, the system matrix is sparse. Like the flowfield case, Eq. (6) must take into account the appropriate conditions at the boundaries.

Coupling

As a result of aerodynamic loads, the equivalent plate representing the wing will deflect; and through bending and twisting of the wing such deflections will perturb the section angles of attack and camber line shapes. These deflections in turn will induce different load distributions and the two processes must be fully interacted until a converged solution is obtained.

The coupling between the structural and the flowfield solutions is achieved through the wing boundary conditions and is included by simply adding the structural deflections to the ordinates of the wing. This coupling is only carried out at the field variables level. In other words, for a linear case (much below the critical Mach number), a case in which the sensitivity matrix $\partial R/\partial\phi$ would not be influenced by the values of ϕ, this aeroelastic coupling would only slightly affect the aerodynamic and the structural sensitivity derivatives. Thus, the flowfield variables and deflections are fully coupled, whereas the sensitivity derivatives are not.

System Sensitivity

As mentioned, for an optimization process to be accurate, it must take into account the system sensitivity derivatives for the coupled disciplines. Thus, the calculation of interdisciplinary sensitivities such as the sensitivity of the pressure distribution to the thickness of the plate or that of the tip deflections with respect to the camber at the tip are needed. In general, the set of equations governing the entire coupled system can be written as[11]

$$A[(\boldsymbol{XD}, \boldsymbol{\delta}), \boldsymbol{\phi}] = 0 \qquad (7)$$

$$S[(\boldsymbol{XD}, \boldsymbol{\phi}), \boldsymbol{\delta}] = 0 \qquad (8)$$

where Eq. (7) represents the aerodynamics and Eq. (8) is for

the structures. For the system analysis ϕ can be replaced by ΔC_p since it is the variable involved in the aerodynamic coupling. The vectors grouped in the inner parentheses are the input, while the vectors of unknowns (output) are listed last. The purpose of the analysis is to find the total derivatives $d\boldsymbol{Y}/d\boldsymbol{XD}$ of the output vector with respect to the different design variables. According to the implicit functions theorem, the previous equations can be written as[11]

$$\Delta C_p = \Delta C_{pA}(\boldsymbol{XD}, \boldsymbol{\delta}) \tag{9}$$

$$\delta = \delta_S(\boldsymbol{XD}, \boldsymbol{\Delta C_p}) \tag{10}$$

After considering $Y = (\{\Delta C_p\}, \{\delta\})$, taking its total derivatives with respect to $\boldsymbol{XD}$, and rearranging the terms, the following system equation is obtained:

$$\begin{bmatrix} I & -J_{AS} \\ -J_{SA} & I \end{bmatrix} \left\{\frac{d\boldsymbol{Y}}{d\boldsymbol{XD}}\right\} = \left\{\frac{\partial \boldsymbol{Y}}{\partial \boldsymbol{XD}}\right\} \tag{11}$$

where, for selected points on the wing, J_{AS} is a Jacobian of the partial coupling sensitivity derivatives $\partial \Delta C_p/\partial \delta$ and J_{SA} is the Jacobian of $\partial \delta/\partial \Delta C_p$. For example, the ith column of J_{AS} comprises the partial derivatives with respect to the ith displacement. The partial derivatives in the coupling matrix as well as the right-hand side are, by definition, calculated using strictly discipline derivatives. Again, the quasianalytical approach is used. Equations (2) and (5) are rewritten as

$$R_{i,j,k} = R_{i,j,k}[(\boldsymbol{XD}, \boldsymbol{\delta}), \phi_{l,m,n}] \tag{12}$$

$$T_{i,k} = T_{i,k}[(\boldsymbol{XD}, \boldsymbol{\Delta C_p}), \delta_{l,n}] \tag{13}$$

where δ is considered an independent variable for Eq. (12) and ΔC_p is considered independent for Eq. (13). This approach is valid since it is discipline specific. Differentiating Eq. (12) with respect to a given deflection and Eq. (13) with respect to a given ΔC_p on the wing yields the system of linear coupling sensitivity equations:

$$\frac{dR_{i,j,k}}{d\delta} = \left[\frac{\partial R_{i,j,k}}{\partial \phi_{l,m,n}}\right] \left\{\frac{\partial \phi_{l,m,n}}{\partial \delta}\right\} + \left\{\frac{\partial R_{i,j,k}}{\partial \delta}\right\} = 0 \tag{14}$$

$$\frac{dT_{i,k}}{d\Delta C_p} = \left[\frac{\partial T_{i,k}}{\partial \delta_{l,n}}\right] \left\{\frac{\partial \delta_{l,n}}{\partial \Delta C_p}\right\} + \left\{\frac{\partial T_{i,k}}{\partial \Delta C_p}\right\} = 0 \tag{15}$$

which when solved yield the coupling sensitivity derivatives, i.e., the elements of the J_{AS} and J_{SA} matrices, necessary for the calculation of the system sensitivities via Eq. (11). Note that in these equations each δ and ΔC_p is considered a design variable. Thus, when computing system sensitivities, the number of effective design variables is augmented by 2 × (number of grid points on the wing) and much of the computational effort involves determining the elements of J_{AS} and J_{SA}.

Design Variables

Design variables are classified into two groups, the aerodynamic variables termed ***XDA*** and the structural variables called ***XDS***. One variable, M_∞, is common to both vectors. A design variable is considered aerodynamic or structural depending in which of the discipline residuals it appears. For example, the angle of attack would be an aerodynamic variable, while the plate thickness, which only appears in the deflection equation, would be a structural variable. However, all of the design variables considered are basic variables in that they are uncoupled and independent. For the current problem the vector of design variables consists of 12 variables that can be classified into three groups:

1) Freestream design variables: these include M_∞ and α. M_∞ enters the formulation through Eq. (1), whereas α appears via its boundary conditions.

2) Cross-sectional design variables: these include the variables that define the wing. For the present study only NACA four-digit airfoils are considered; and the relevant design variables are *TH*, *C*, and *LC* at the root and tip and T_{tip}. The airfoil sections as well as the aerodynamic twist at a given span station are obtained by linear lofting between the root and tip the values for twist, *TH*, *C*, and *LC*. It should be noted that this formulation is not a point-by-point lofting in which the vertical coordinate is interpolated linearly from root to tip, but was chosen to simplify the analytical derivations as well as the coding. With this approach, the vector of the aerodynamic design variables can be written:

$$\boldsymbol{XDA} = (\alpha, TH_{root}, TH_{tip}, C_{root}, C_{tip}, LC_{root}, LC_{tip}, T_{tip}, M_\infty) \tag{16}$$

3) The structural variables: these include the parameters M_∞, t, ν, and E involved in the plate deflection equation. Thus, the vector of structural design variables is

$$\boldsymbol{XDS} = (M_\infty, t, \nu, E) \tag{17}$$

These two vectors are combined to form a single vector of design variables:

$$\boldsymbol{XD} = (\alpha, TH_{root}, TH_{tip}, C_{root}, C_{tip}, LC_{root}, LC_{tip}, T_{tip}, M_\infty, t, \nu, E) \tag{18}$$

Approach and Numerical Procedure

Aeroelastic Coupling and System Sensitivity Analyses

Aerodynamic-structural coupling can be carried out at two levels, defined here to be zero and first order. The zero-order coupling corresponds to an updating of the aerodynamic boundary conditions each time after the structural deflections are calculated and vice versa. However, sensitivities are computed as discipline sensitivities and do not directly include the complete effects of aerodynamic-structural coupling. On the other hand, the first-order coupling is defined to mean that the effect of the structure on the flowfield and vice versa is taken into account not only at the flowfield-deflection level, but also at the sensitivity level. For example, for the zero-order coupling the structural deflections affect the aerodynamic sensitivity derivatives through the spanwise flow component ϕ_z in $\partial \boldsymbol{R}/\partial \boldsymbol{XDA}$, whereas the first-order coupling also affects that expression through a coupling term $\partial \phi_z/\partial \delta$. This term is called a coupling sensitivity. In this second case, the deflections are not considered constant in the aerodynamic residual expressions [Eq. (7)], as in the discipline specific analysis, and are considered as design variables. Likewise, in first-order coupling, the potentials related to the C_p calculation along the wing are treated as design variables for Eq. (8).

The terms that affect coupling the most are those that appear directly in the residual expressions. These are the deflections, since they enter directly in the boundary conditions for the aerodynamic residuals, and the loads ΔC_p, which appear in the structural residuals. As shown in Eq. (11), the coupling derivatives, $\partial \Delta C_p/\partial \delta$ and $\partial \delta/\Delta C_p$, are the essential components of the system sensitivity matrix and are used to obtain the system sensitivity derivatives. The equations for determining these coupling derivatives are Eqs. (14) and (15). However, in many cases not all of the deflections or loads can be used in the system matrix since such inclusions would require extensive memory storage and CPU times that are unrealistic. Hence, the choice of which loads and deflections to include in the system sensitivity equation is subject to judgment and experimentation.

Numerical Approach

The coefficient matrices associated with the linear sensitivity equations, as well as those resulting from the finite differencing of the flowfield and structural solutions, are generally very sparse. Thus, the solution of the corresponding linear equations by standard direct solvers is memory inefficient and iterative methods should be considered.[5-7] In addition, since the nonlinear flowfield equations must be solved iteratively, the use of a similar iterative scheme to obtain the sensitivities would seem appropriate.

A possible scheme is the incremental iterative technique,[3,7] which has exhibited better convergence characteristics in many cases than standard iterative techniques. This method involves a formulation in which a system of algebraic equations has the general form[7]:

$$[A]\{Z^*\} + \{B\} = \{0\} \tag{19}$$

where $\{Z^*\}$, the solution vector, is obtained by the two-step formulation:

$$\begin{aligned} -[A^*]\{\Delta^n Z\} &= [A]\{Z^n\} + \{B\} \\ \{Z^{n+1}\} &= \{Z^n\} + \{\Delta^n Z\} \end{aligned} \tag{20}$$

Here, n is the iteration index and $[A^*]$ is a convenient approximation for $[A]$, generally chosen to enhance diagonal dominance and the convergence characteristics of the system.

The previous formulation, when applied to sensitivity equations, can require the storage of a large sensitivity matrix, even when the zero elements are excluded. However, the use of a point algorithm to obtain the increments avoids that problem since it only requires the elements of the matrix relevant to the calculation of the increment at point i, j, k. While such an approach has the possible disadvantage of slower convergence, the sensitivity equations are linear and their convergence should be similar to that of the nonlinear flowfield.

An example of such a point algorithm is the semi-implicit Zebra scheme,[12] which mimics point successive over relaxation. The algorithm marches in the streamwise direction solving by spanwise planes. In each plane, the points where $j + k$ are odd are denoted black and the ones where $j + k$ are even are denoted white. Each plane is solved by a two-pass sweep in which new black values are obtained first, followed by the white ones. Convergence is accelerated because calculations at the white points use updated values at the black points. Because of its uncoupled formulation, this method is suitable for sequential, vector, and parallel machines.

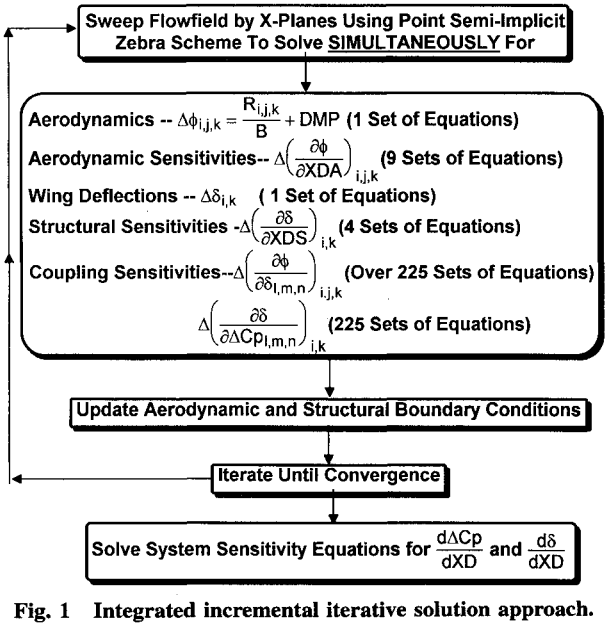

Fig. 1 Integrated incremental iterative solution approach.

In the Zebra algorithm, because of the point semi-implicitness, the matrix $[A^*]$ is reduced to a scalar B. Hence, the incremental changes in the unknowns can be found straightforwardly. For example, for the aerodynamic potential

$$\Delta\phi_{i,j,k} = (R_{i,j,k}/B) + DMP \tag{21}$$

where DMP is a damping term added for stability.[12] The same type of formulas can also be used to calculate the increments for the aerodynamic sensitivity field variables, structural deflections, structural sensitivity derivatives, and coupling derivatives.[10] The algorithm used is schematically described in Fig. 1.

Discussion of Results

The wing configuration considered in this study had a rectangular planform of constant unit chord and a half-span value of $z_{tip} = 1.58$, an AR of 3.17 with a root-to-tip twist of -1 deg, and the root and tip airfoil sections were NACA 2406 and NACA 1706, respectively. The freestream conditions were $M_\infty = 0.82$ with $\alpha = 2$ deg, and the equivalent flat plate structural parameters were $t = 0.02$, $E = 1 \times 10^7$, and $\nu = 0.33$. The case presented here used a $97 \times 16 \times 16$ grid for the flowfield and 49×10 for the structural deflections. The freestream Mach number is supercritical and a shock wave is present on the inboard sections of the upper surface of the wing. However, the shock wave disappears on the outboard sections due to three-dimensional effects. Thus, this Mach number is interesting because it locally includes both subcritical and supercritical behavior of the flowfield and the corresponding sensitivities. Results[10] were computed for equivalent plate thicknesses of 5 and 2%, but only the 2% results are shown. A 1% thick case was also attempted, but it was aeroelastically divergent.

For these proof-of-concept investigations, an arbitrarily large number of iterative cycles was performed to ensure that all residuals had been reduced as much as possible and to establish that they subsequently remained unchanged for several hundred cycles. The total number of iterations often was several thousand; and no attempt was made to optimize the number of cycles or the computational time. Typically, the residuals for the nonlinear aerodynamic solution were reduced four to six orders of magnitude, while those for the deflections, aerodynamic and discipline sensitivities, and coupling derivatives were lowered three to four orders of magnitude. Further, in the early stages of the study, sensitivities were computed by both the quasianalytical and the finite difference approach. These studies along with previous results[4,5] verified the accuracy of the present quasianalytical scheme.

For the coupling variables needed to determine the system sensitivities, many cases were studied, but only two are discussed here. The first used 8 of the 10 spanwise stations with each involving 25 of the 49 possible chordwise points. The root station was ignored since it has zero deflections and the next to last span station near the wingtip was excluded. Further, the points selected for the chordwise coupling derivative distribution did not include points near the trailing edge. The second, whose results are displayed in the figures, used nine spanwise stations, again with 25 chordwise points and the root station excluded. In this case, the coupling derivatives were computed at points near the wing trailing edge. It is believed, since it is numerically difficult to include every point used in the fine grid, that the deflections and loads selected for the coupling system coefficients in the sensitivities are representative. However, these choices may need further investigation.

Figure 2 shows the pressure distribution at 2 of the 10 spanwise stations. The upper surface shows a shock wave at approximately $x = 0.5$ in the sections near the root. The airfoil

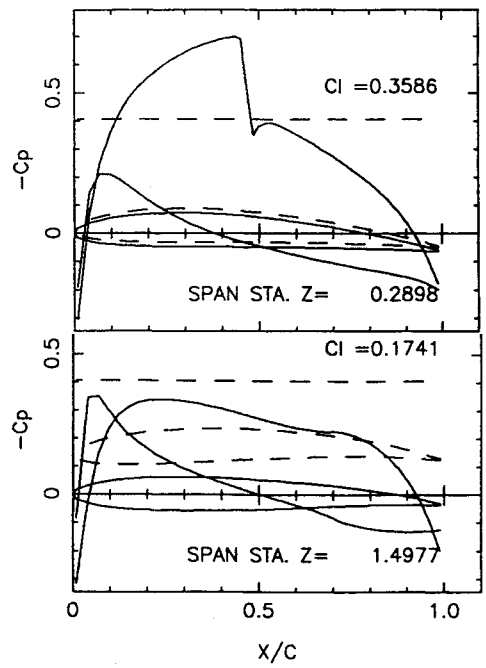

Fig. 2 C_p distribution and original and deflected wing shape at two span stations.

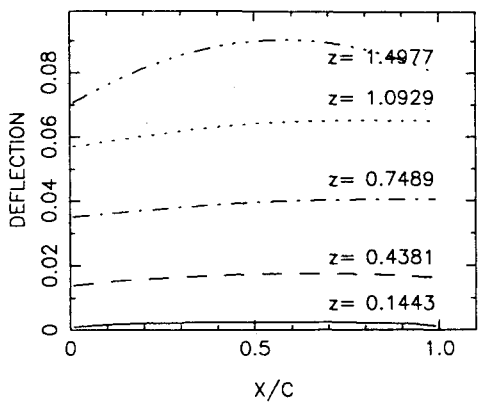

Fig. 3 Structural deflection of equivalent plate.

section, being nonconstant from root to tip, is also shown on the same diagram; and the angle of attack as well as the geometric twist are taken into account when plotting the geometry. The final deflected shape of the airfoil due to aeroelastic coupling is portrayed in dashed lines, but not to scale. The critical pressure coefficient level C_p^* is also shown, and comparison of C_p^* with the pressures indicates that the shock wave weakens progressively when approaching the tip, which is obviously subcritical. At the tip, the pressure distribution is typical of a subcritical aft-cambered NACA section. Note that due to the change in airfoil sections from root to tip the wing has some inherent aerodynamic twist and that the lower surface C_p curve at the tip section is above the upper one, causing negative aerodynamic loading at the leading edge.

Figure 3 shows the structural deflection of the equivalent plate at different span stations. Notice that a line drawn from the leading to the trailing edge of the plate at each section would form an angle of attack with the x axis, which would be an induced twist due to structural deflection. Furthermore, even though the amplitudes are extremely small, bending exists in the sections. This cambering effect due to chordwise bending is more pronounced as the tip is approached. In fact, the chordwise section of the equivalent plate near the tip looks like a camber line that could cause an increase in lift and could become an important component of the tip aerodynamics. Note that the maximum of the structurally induced camber is slightly aft of midchord.

While sensitivity derivatives for all of the design variables were obtained at all span stations, they cannot all be included due to space limitations. Representative results for aerodynamic discipline sensitivity derivatives are shown in Figs. 4 and 5, while some of the system sensitivity derivatives are shown in Figs. 6–12. Additional results for both discipline and system aerodynamic and structural derivatives are given in Refs. 9 and 10.

Figure 4 represents the results for the sensitivity with respect to the angle of attack at both a supercritical and a subcritical station. Both upper and lower surface results are shown as well

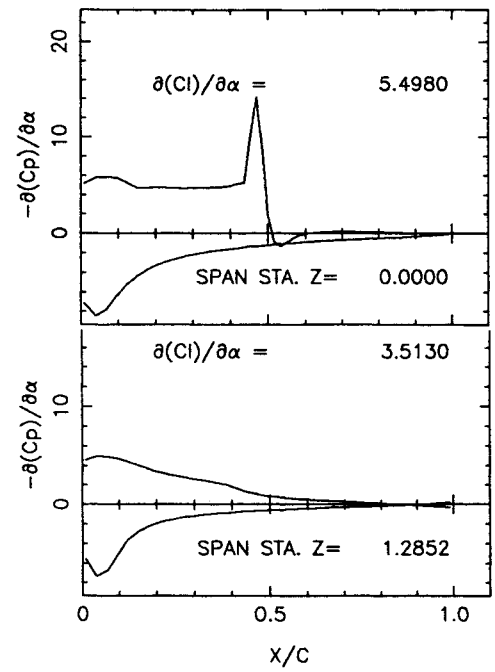

Fig. 4 Discipline result for C_p sensitivity to α at two span stations.

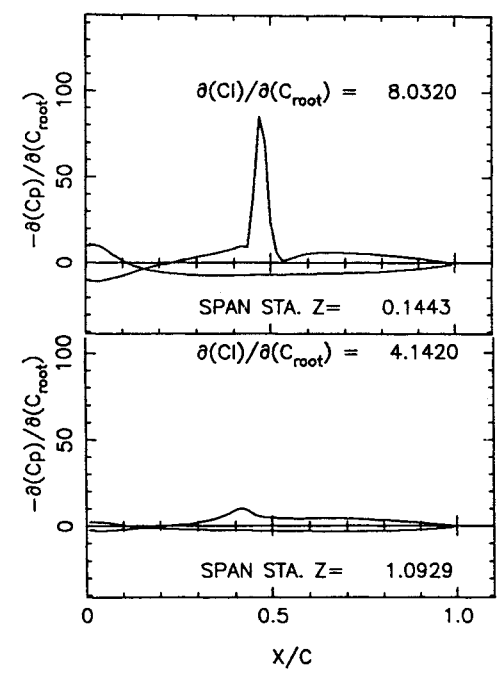

Fig. 5 Discipline result for C_p sensitivity to root camber at two span stations.

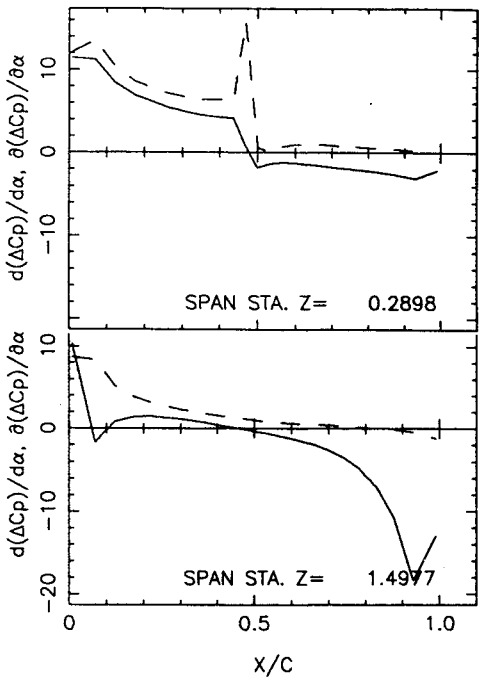

Fig. 6 ΔC_p **sensitivity to** α**; discipline result dashed, system result solid.**

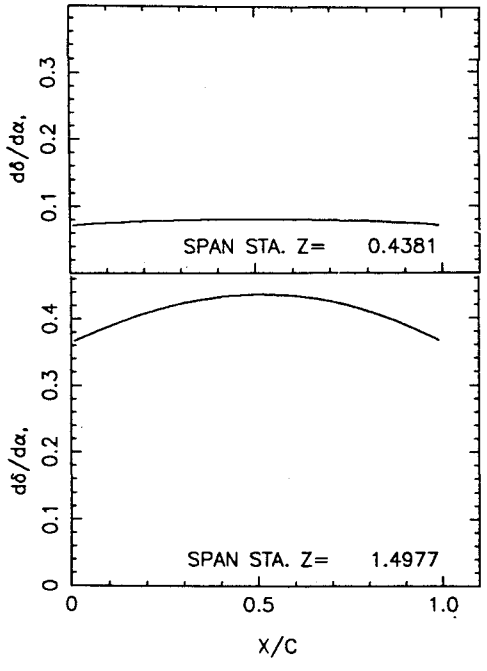

Fig. 7 System deflection sensitivity to α**.**

as the local lift coefficient sensitivities, and as expected,[4] the upper and lower results are similar, but of opposite sign. Note that the inboard upper surface values exhibit a discontinuity or spike near the shock wave, which reflects the sensitivity of C_p to shock movement with α.

Figure 5 shows the results for the sensitivity with respect to root camber at two supercritical stations, one with a strong shock and one almost shockless. Note that the lift coefficient sensitivity with respect to camber is quite large, implying that the camber derivative would be very important in any optimization. While not shown, the sensitivity to the location of maximum root camber was significantly smaller,[10] indicating that camber location is not a strong design variable.

The aerodynamic system sensitivity results with respect to angle of attack are shown in Fig. 6 at two different stations. The dashed curves correspond to the discipline sensitivities and the solid curves are the system values. The results differ mostly around the leading and trailing edges as the wingtip is approached since an angle of attack increase would induce additional structural deflections not included in the aerodynamic discipline derivatives and small changes, particularly near the trailing edge, strongly affect the pressures. Note that the system and discipline derivatives differ not only in magnitude, but also in sign over the aft portion of the wing. It appears that in predicting pressure changes over the aft portion of the wing that discipline sensitivities would be inaccurate and that system derivatives are essential. Note that the system

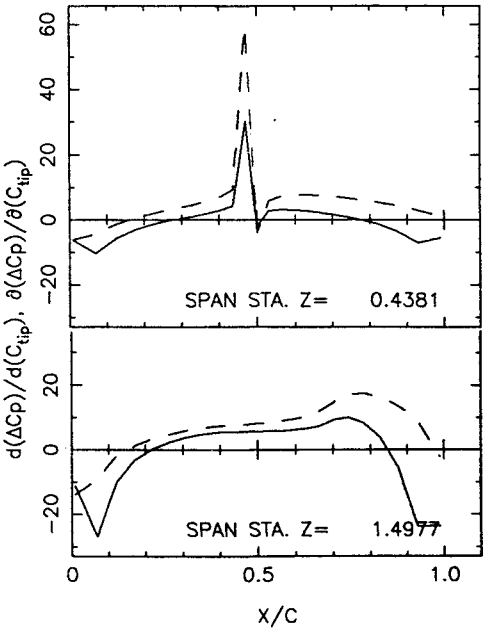

Fig. 8 ΔC_p **sensitivity to tip camber; discipline result dashed, system result solid.**

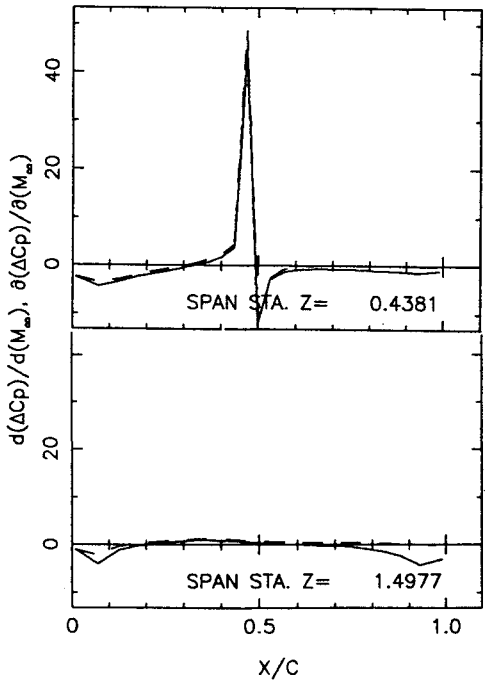

Fig. 9 ΔC_p **sensitivity to** M_∞**; discipline result dashed, system result solid.**

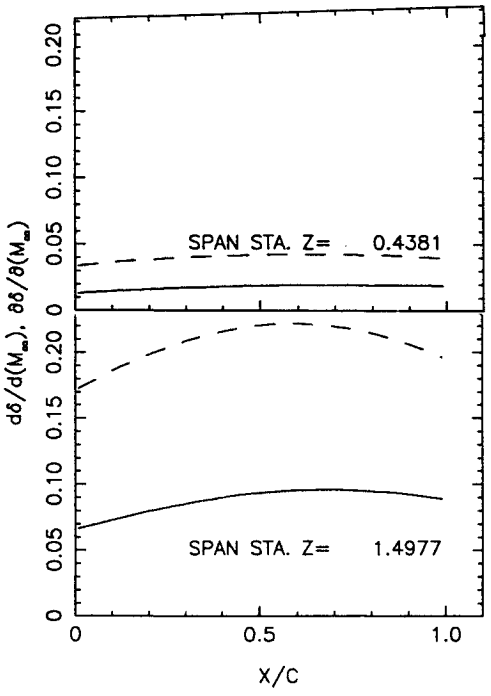

Fig. 10 Deflection sensitivity to M_∞; discipline result dashed, system result solid.

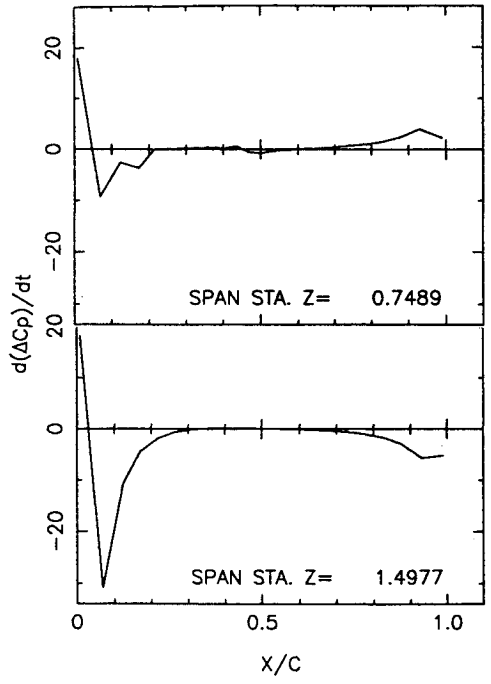

Fig. 11 System ΔC_p sensitivity to equivalent plate thickness.

derivatives do change slope and approach zero as the trailing edge is approached, as required by theory.

The system structural sensitivities, $d\delta/d\alpha$, which cannot be obtained from a discipline approach, show on Fig. 7 that, as expected, the wing will deflect more with increased angle of attack. However, near the wingtip, an angle-of-attack increase will induce some additional structural cambering. These values for $d\delta/d\alpha$ mean about a 1.5% increase in the deflections for a 10% increase in α, which while not large, might be important during optimization.

Interestingly, when the coupling sensitivities were computed excluding at each span station the point next to the trailing edge, the system $d\delta/d\alpha$ curves had negative values. The omission of crucial information near the trailing edge yielded larger values for $d(\Delta C_p)/d\alpha$ near the trailing edge and did not detect the required turnaround and approach to zero. As a result, the decrease in loading effect near the trailing edge was overemphasized, and the system derivatives predicted negative derivatives and less deflection. Obviously, the locations selected for computing coupling sensitivities must be chosen to include details near the trailing edge of the wing.

Two aerodynamic system sensitivity results with respect to camber at the tip are shown in Fig. 8. This case exhibits significant differences in magnitude, character, and sign between the discipline and system aerodynamic derivatives, particularly in the trailing-edge region where the system derivatives indicate up to a 20% decrease in loading for a 10% tip camber increase while the discipline sensitivities would predict an increase.

System sensitivities with respect to Mach number, which is a discipline design variable for both aerodynamics and structures, are shown in Figs. 9 and 10. Here, the aerodynamic system and discipline sensitivities are essentially identical, except on the aft quarter of the wing, which means that good estimates for the changes in aerodynamic loading with Mach number can be obtained from discipline derivatives over much of the wing. However, while the structural discipline derivatives are positive, indicating that an increased Mach number will increase ΔC_p loads, and thus, the deflections, the structural system derivatives are significantly smaller than and do not increase as rapidly with span as do the discipline values. This behavior can be explained by the system load sensitivities, which are negative near the leading and trailing edges. Thus, as Mach number increases, the loadings near the leading and trailing edges will decrease, the increase in structural cambering will be less than predicted by the structural discipline sensitivity, and the overall increase in aerodynamic loading will be less resulting in less deflection. This behavior is evident by comparing the discipline $\partial\delta/\partial M_\infty$ and system results $d\delta/dM_\infty$ at station $z = 1.49$.

All of the pure structural design variables (i.e., t, ν, and E) behave similarly. For simplicity, results are only shown on Figs. 11 and 12 at two stations for the thickness design variable. In this case, the system $d(\Delta C_p)/dt$ sensitivities show that

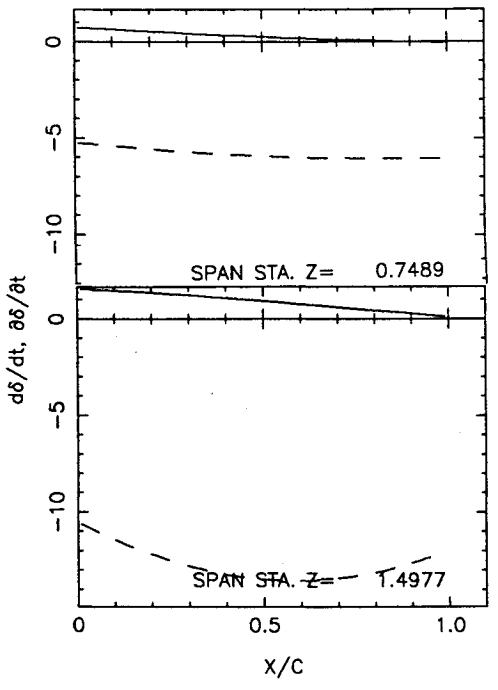

Fig. 12 Deflection sensitivity to equivalent plate thickness; discipline result dashed, system result solid.

near the leading edge an increase in wing equivalent structural thickness will lead to an unloading and that near the trailing edge it will cause either an increased loading or an unloading less than that near the leading edge, depending upon span location. However, the discipline deflection sensitivities, $\partial\delta/\partial t$, show decreased deflection and a decrease in structural cambering with increased thickness. The latter is indicated by the more negative values of $\partial\delta/\partial t$ at midchord and at the trailing edge than at the leading edge; and the effect is more pronounced with span. On the other hand, the system sensitivity values for $d\delta/dt$ exhibit little variation with span, are by comparison small, and predict a positive deflection, particularly near the leading edge. Here the system derivatives reflect the fact that an increase in thickness will decrease the leading-edge load more than the trailing edge, which will three dimensionally change the structural cambering and the structural induced angle of attack. The system derivatives $d\delta/dt$ indicate that the latter will dominate and that the wing will actually deflect and twist upward slightly. In this case, and similarly for the design variables ν and E, the system response is contrary to intuition and would not be predicted correctly by only considering discipline sensitivities. Thus, it appears that in many cases, proper sensitivities can only be obtained by computing system derivatives.

In the early stages of this study, system sensitivities were computed from the full flowfield ($97 \times 16 \times 16$) and structural (49×10) solutions using coupling sensitivities computed at only eight span stations, each having 13 chordwise coupling points. The resultant system derivatives often differed in magnitude and sometimes sign from those presented here that were computed using nine span stations each with 25 chordwise coupling points. These differences can be explained by the fact that the choice of 25 coupling points per station will describe the shock more accurately. Obviously, based upon this result and those discussed earlier concerning the importance of including coupling sensitivities in the trailing-edge region, the number and location of coupling sensitivities is important and needs further investigation.

Conclusions

Based on the results presented, the incremental–iterative technique combined with the semi-implicit ZEBRA algorithm is a feasible, successful, and memory-efficient approach for calculating transonic aerodynamics, structural deflections, and the sensitivity and coupling derivatives obtained from the quasianalytical formulation. Large memory for the storage of the sensitivity matrices is not needed, and the sensitivity and coupling derivatives can be calculated at the same time as the flowfield and deflections, instead of using converged solutions as input to sparse matrix solvers.[5] The computational resources thus saved can be used for finer grids, more design variables, and additional disciplines.

In the present study, a transonic small perturbation solver was coupled with an equivalent thin plate model along with quasianalytical formulations for the disciplinary design sensitivities and the interdisciplinary coupling derivatives. This static aeroelastic coupling is potentially efficient since the structural calculation and aerodynamic, structural, and coupling sensitivities are computed at the same time as the flowfield with the same incremental iterative technique.

Because this aeroelastic system is multidisciplinary, system sensitivity derivatives were also computed to account for the influence of each discipline on the other. The resultant system sensitivities often exhibited significant differences in magnitude and sometimes sign from the discipline derivatives. Such differences could be very important in any subsequent optimization process. In addition, the system results were sensitive to the number and location of the coupling sensitivity derivatives, particularly near the trailing edge of the wing. Since the coupling derivatives are not computationally easy to obtain due to slow convergence (especially for the sensitivity of δ with ΔC_p), more studies are needed on the number and location of the coupling points chosen to describe the system behavior. Further, it was noticed for some design variables that the system sensitivity results did not differ significantly from the discipline results. For these cases, the discipline sensitivities could be used in an optimization process, thus simplifying computational effort.

Acknowledgments

This work was primarily supported by the Aerospace Engineering Department of Texas A&M University. Computer support was also provided by the office of the Associate Provost for Computing.

References

[1]Adelman, H. M., and Haftka, R. T., "Sensitivity Analysis and Discrete Structural Systems," *AIAA Journal*, Vol. 24, No. 5, 1986, pp. 823–832.

[2]Bristow, D. R., and Hawk, J. D., "Subsonic Panel Method for Designing Wing Surfaces from Pressure Distributions," NASA CR-3713, July 1983.

[3]Korivi, V. M., Taylor, A. C., III, Newman, P. A., Hou, G. W., and Jones, H. E., "An Incremental Strategy for Calculating Consistent Discrete CFD Sensitivity Derivatives," NASA TM 104207, Feb. 1992.

[4]Elbanna, H. M., and Carlson, L. A., "Determination of Aerodynamic Sensitivity Coefficients Based on the Transonic Small Perturbation Formulation," *AIAA Journal*, Vol. 27, No. 6, 1990, pp. 507–515.

[5]Elbanna, H. M., and Carlson, L. A., "Aerodynamic Sensitivity Coefficients Using the Three-Dimensional Full Potential Equation," *Journal of Aircraft*, Vol. 31, No. 5, 1994, pp. 1071–1077.

[6]Baysal, O., Eleshaky, M. E., and Burgreen, G. W., "Aerodynamic Shape Optimization Using Sensitivity Analysis on Third-Order Euler Equation," AIAA Paper 91-1557, June 1991.

[7]Korivi, V. M., Taylor, A. C., III, Newman, P. A., Hou, G. W., and Jones, H. E., "An Approximately Factored Incremental Strategy for Calculating Consistent Discrete Aerodynamic Sensitivity Derivatives," AIAA Paper 92-4746, Sept. 1992.

[8]Sobieszczanski-Sobieski, J., "Multidisciplinary Optimization for Engineering Systems: Achievements and Potential," NASA TM 101566, March 1989.

[9]Arslan, A. E., "Analysis and Numerical Computation of Sensitivity Derivatives in the Transonic Regime," M.S. Thesis, Texas A&M Univ., College Station, TX, Dec. 1993.

[10]Arslan, A. E., and Carlson, L. A., "Integrated Determination of Sensitivity Derivatives for an Aeroelastic Transonic Wing," AIAA Paper 94-4400, Sept. 1994.

[11]Sobieszczanski-Sobieski, J., "Sensitivity of Complex Coupled Systems," *AIAA Journal*, Vol. 28, No. 1, 1990, pp. 153–160.

[12]Weed, R. A., Anderson, W. K., and Carlson, L. A., "A Direct-Inverse Three Dimensional Transonic Wing Design Method for Vector Computers," AIAA Paper 84-2156, Aug. 1984.